A mathematical analysis of an extended model describing sea ice-induced frequency lock-in for vertically sided offshore structures

Abramian, Andrei K.; Vakulenko, Sergei A.; Horssen, Wim T.van

DOI
10.1007/s11071-021-07089-5

Publication date
2021

Document Version
Final published version

Published in
Nonlinear Dynamics

Nonlinear Dyn (2022) 107:683–699
https://doi.org/10.1007/s11071-021-07089-5

ORIGINAL PAPER

A mathematical analysis of an extended model describing sea ice-induced frequency lock-in for vertically sided offshore structures

Andrei K. Abramian · **Sergei A. Vakulenko** · **Wim T. van Horssen**

Received: 23 August 2021 / Accepted: 18 November 2021 / Published online: 24 December 2021

Abstract This paper presents a mathematical analysis of an extended model describing a sea ice-induced frequency lock-in for vertically sided offshore structures. A simple Euler–Bernoulli beam as model for the offshore structure is used, and a moving boundary between an ice floe and the structure itself is introduced. A nonlinear equation for the beam dynamics is found by using an asymptotical approach and a Galerkin procedure. It is shown analytically that a frequency lock-in regime occurs during ice-induced vibrations (IIV), when the dominant ice force frequency is closed to a natural frequency of the structure. For beams, perturbed by small nonlinearities and a small damping, the concept of quasi-modes is introduced. A quasi-mode is a linear combination of the usual eigenmodes. The large time behaviour of solutions at the instability onset is determined by a single quasi-mode, which is maximally linearly unstable.The beam model analysis leads to the conclusion that an interaction between a moving ice floe and a structure can lead to a "negative friction" for particular values of the ice floe parameters. From the analysis presented in the paper it follows that the lock-in regime occurs when simultaneously two phenomena are present: a forcing resonance and a "negative friction".

Keywords Ice induced vibration · Lock-in · Quasi-mode · Negative friction · Moving contact

A. K. Abramian (✉) · S. A. Vakulenko
Institute for Problems in Mechanical Engineering, Saint Petersburg, Russia
e-mail: andabr55@gmail.com; abr33@yahoo.co.uk

W. T. van Horssen
Faculty EEMCS, Delft Institute of Applied Mathematics, Delft University of Technology, Mekelweg 4, 2628 CD Delft, The Netherlands
e-mail: W.T.vanHorssen@tudelft.nl

List of symbols

$w = w(z,t)$	Transverse displacement of the beam
z	Vertical coordinate (along the beam axis)
x	Horizontal coordinate (along the ice rod axis)
$-H_1$	Coordinate of the lower edge of the beam
H_2	Coordinate of the top of the beam
t	Time
subscripts z, x, t	Indicating partial derivatives with respect to z,x and t, respectively
D	Beam bending rigidity
m_0	Beam mass per unit length
$\alpha > 0$	Viscous damping coefficient of the beam material
μ	Force acting on the beam due to the ice rod
$u = u(x,t)$	Longitudinal ice rod displacement
E	Ice Young's modulus

F	Ice rod cross sectional area
δ_0	Ice rod damping coefficient
$m > 0$	Ice rod mass per unit length
Q	Force occurring in the rod due to its side-surface contact with others ice rods
β	Ice friction coefficient during its side-surface contact
r	Coefficient relating the shearing strain in the ice rod
k_0	Characterizes the rod compression which is caused by stresses due to the ice rod compression in the transverse direction by other ice rods
h	Ice rod thickness
γ	Coefficient determining the rate of decrease of the displacement u over the ice rod length
ν	Poisson ratio
$s(t)$	The total shift of the ice rod
$v > 0$	Relative ice velocity
$\rho(t)$	Shift of the ice rod as a result of ice breaking
d	Length of an ice block that split off the ice rod, each time it breaks
t_n	Time instants when the ice rod crushes
$H(z)$	Heaviside step function
p	Pressure in the ice
p_c	Critical pressure in the ice when it breaks
$c_0 = \sqrt{r/m}$	Ice sound velocity
$\epsilon = k_0/c_0^2 F$	Small parameter
Ω_n	Natural frequencies of the beam
$\tau = \epsilon t$	Slow time
λ_n	Eigenvalues of the initial-boundary value problem
$\omega = 2\pi v/d$	Breaking frequency of an ice rod
A_n	Amplitude of the n-th oscillation mode of the beam
ϕ_n	Phase of the n-th oscillation mode of the beam
$A = (A_1, A_2, \ldots)$	Infinite sequences of the functions $A_n(\tau)$
$\phi = (\phi_1, \phi_2, \ldots)$	Infinite sequences of the functions $\phi_n(\tau)$
$\|A\|$	Average amplitude of the beam vibration
i	Unit imaginary number

1 Introduction

Bottom fixed offshore structures subjected to dynamic loading due to drifting ice may experience large amplitude vibrations. The reason for this undesirable behavior is the phenomenon of ice-induced vibrations (IIV), and in particular its frequency lock-in (FLI) regime. The FLI regime starts when the ice force frequency is close to a natural frequency of the structure. The IIV phenomenon includes 3 regimes: an intermittent crushing, a continuous brittle crushing, and a FLI which is the most dangerous from the practical point of view. The amplitudes of vibrations during an intermittent crushing and continuous brittle crushing are smaller than those in the FLI regime. The physical mechanism of IIV is nowadays explained by two theories: the force vibration theory, and the self-excited vibration theory. The first theory indicates that steady IIV regimes depend on the breaking frequency of the ice sheets [22,29,33]. The second theory explains the initiation of the steady regimes by negative damping occurring during an ice structure interaction [5,23]. Based on experiments and field observations some new coupled models for IIV were developed [1,2,9,12,14,16,21,25,33]. In these models the structure is usually described as a one or a two degree of freedom oscillator with a linear or nonlinear structure rigidity. Depending on the IIV model, a linear or nonlinear rheological model for the ice was chosen. Only a few models exist which describe the structure as a continuous structure. The flexibility of a structural model is usually represented through a finite number of assumed modes [8,11,19,27,32,37]. The models introduced in the aforementioned papers lead to a system of nonlinear ODEs that usually is analyzed and solved numerically. A semi-analytical method to approximate the behavior of the structure during a FLI regime is suggested in [32] based on solutions of the ODEs. The physical mechanism of the FLI was analysed in [18] by incorporating the Van der Pol equation into the model of IIV.

This paper proposes an analytical analysis of a new model. The model assumes that both the structure and the ice floe are continuous mechanical systems with a moving contact between the beam and the ice. By extending existing models we incorporate this moving contact in the analysis of the beam and the ice floe

dynamics. The novelty with respect to existing models is that the function which describes the movement of this contact is not prescribed but unknown, and should be found. By considering continuous models for the interacting structure and ice, gives us a possibility to describe the appearance of a second oscillation mode of the structure during their interaction. Existing models are not providing such a possibility. A nonlinear ODE for the beam dynamics is finally obtained and investigated with the help of an asymptotic approach. The following results are obtained. An asymptotic formula shows how the negative friction depends on the relative ice velocity and other system parameters. We show that a frequency lock-in regime is a result of a simultaneous action of two physical mechanisms: a forced resonance and a negative friction. First, a resonance of the structure caused by regular breaking of the ice floe occurs. Then, for a particular value of the ice floe velocity this resonance leads to a negative friction. As a result the amplitude of the structure vibration becomes large.The structure instability occurs at the two first natural frequencies of the beam. We observe two pitchfork bifurcations, a direct one leading to the instability onset, and an inverse one, which produces damping.

This paper is organised as follows. In Sect. 2 of this paper the problem is formulated, and in Sects. 3 and 4 the problem is solved approximately by using asymptotic methods. In Sect. 5 asymptotic expressions for the ice rod displacement are found. Stability issues and resonances are discussed in Sect. 6, and finally in Sect. 7 some conclusions are drawn.

2 Statement of the problem

In this section of the paper an Euler–Bernoulli beam model for an offshore structure interacting with an ice floe is formulated. The most important symbols which are used in this paper are the following one.

As suggested in [2,12] the ice floe is considered as a system of ice rods. Considering only one rod follows from the theory introduced in [35]. It is also assumed that the ice during the FLI regime is always in contact with the structure as suggested in [12]. A vertical beam and a moving ice rod are shown schematically in Fig. 1. Based on these assumptions, the equation describing the beam dynamics is given by:

$$Dw_{zzzz} + m_0 w_{tt} + \alpha w_{zzzzt} = \mu\delta(z), \tag{1}$$

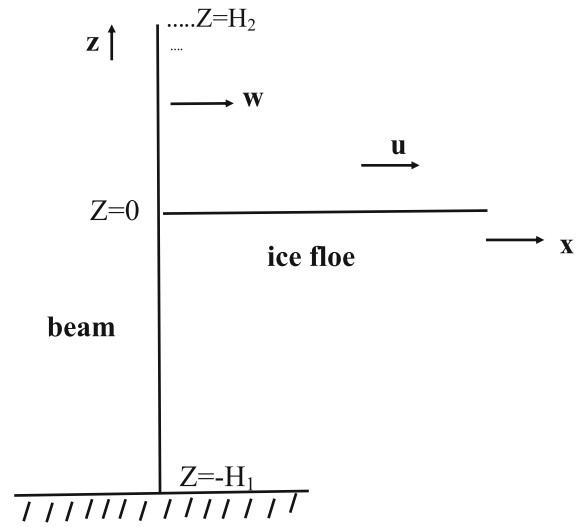

Fig. 1 Dynamic beam model of the ice-structure interaction

where $w = w(z,t)$ is the transverse displacement of the beam, z is a vertical coordinate (along the beam axis), $z \in (-H_1, H_2)$, subscripts z, t are indicating partial derivatives with respect to z and t, D is the bending rigidity of the beam, m_0 is a mass of the beam per unit length, and $\alpha > 0$ is a viscous damping coefficient, and the term αw_{zzzzt} is the Kelvin–Voight damping term, which describes a lateral structural damping. The term $\mu\delta(z)$ simulates the localized action (due to presence of delta-functions) of the ice rod on the platform (beam) at surface level $z = 0$, where μ depends on the state of the ice rod. For Eq. (1), the following initial conditions are used:

$$w(z,0) = 0, \quad w_t(z,0) = 0. \tag{2}$$

The boundary conditions are as follows. We use clamped boundary conditions at the lower edge of the beam at $z = -H_1$:

$$w(z,t) = w_z(z,t) = 0 \tag{3}$$

and the following free end conditions at the top of the beam ([4]) at $z = H_2$:

$$\begin{aligned} &Dw_{zz}(z,t) + \alpha w_{zzt} \\ &\quad = Dw_{zzz}(z,t) + \alpha w_{zzzt}|_{z=H_2} = 0. \end{aligned} \tag{4}$$

The term μ in (1) defines a force acting on the beam due to the ice rod, and this term is given by

$$\mu = \frac{EF}{M}(u_x + \delta_0 u_{xt})\big|_{x=w(0,t)}, \tag{5}$$

where $u = u(x,t)$ is the longitudinal ice rod displacement, subscripts x, t are indicating partial derivatives

with respect to x and t, E is the ice Young's modulus, F is the ice rod cross sectional area, and δ_0 is the ice internal, structural damping coefficient. The term u_x in the right hand side of (5) defines the contribution of linear deformations, and the term u_{xt} is the ice viscosity term. To simplify notations, let us introduce the auxiliary quantity

$$q(t) = w(0,t), \quad q(0) = 0, \quad \left.\frac{dq}{dt}\right|_{t=0} = 0.$$

The boundary conditions at $x = q(t)$ (moving boundary) also can be found in many other problems (see for instance [3,10,30,39]) where, oscillations in axially moving cables are considered. The following equation describes the dynamics of the ice rod, which is defined on the semi-infinite domain $I_t = \{x : q(t) < x < \infty\}$ (see [2,35]),

$$ru_{xx} - mu_{tt} + \delta_0 u_{xxt} = Q, \tag{6}$$

$$Q = -\beta(s_t - u_t) - k_0(s - u), \tag{7}$$

where $u(x,t)$ is the unknown ice rod displacement, $m > 0$ is the ice rod mass per unit length, Q is a force occurring in the rod due to its side-surface contact with others ice rods in the space around the rod in the ice floe that is considered in (6). The ice rod is drifting along the x-axis. The parameters β, r, δ_0, and k_0 are positive. The coefficient β is the ice friction coefficient during its side-surface contact, the coefficient r is the coefficient relating the shearing stress and the strain in the ice rod, and thus defines "the load spreading capacity of the foundation" according to [35]. The parameter k_0 characterizes the rod compression which is caused by stresses due to the ice rod compression in the transverse direction by other ice rods. Note that $r = \frac{Eh}{4\gamma(1+\nu)}$, where h is the ice rod thickness, the parameter ν is the Poisson ratio, the parameter γ is a coefficient determining the rate of decrease of the displacement u over the ice rod length and can be found experimentally (see also [35] for further details). The parameter $k_0 = \frac{Eh\gamma}{2(1-\nu^2)}$. In other words, the ice rod behavior can be modelled by a generalized spring and a generalized dashpot as suggested in [20]. The function $s(t)$ describes the shift of the ice rod, and we suppose that $s(t)$ is defined by

$$s(t) = -vt + \rho(t), \tag{8}$$

where $v > 0$ is the relative ice velocity, and

$$\rho(t) = \sum_{n=1}^{\infty} d_n H(t - t_n). \tag{9}$$

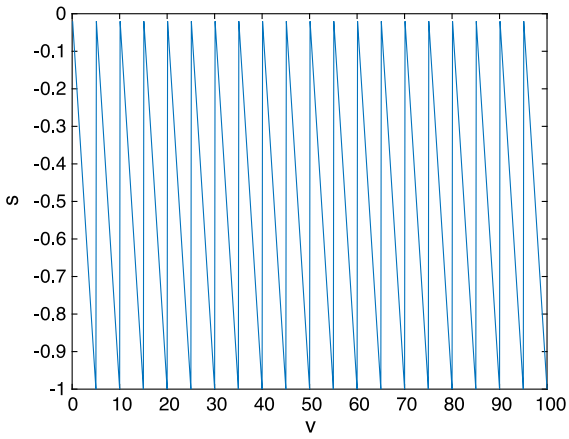

Fig. 2 This plot shows a typical dependence of $s(t)$ on time. The parameter values are $d = d_n = 1$, $\Delta t = t_{n+1} - t_n = 5$, and $v = 0.2$

Here, t_n are time instants when the ice rod crushes at $x = q(t)$; d_n are the lengths of ice blocks that split off, and $H(z)$ stands for the Heaviside step function. See also Fig. 2 for a typical dependence of $s(t)$ on time. The time instants t_n are defined by the condition

$$p(t_n) = p_c, \tag{10}$$

that is, when the pressure p in the ice attains a critical level p_c. The pressure p can be computed by the relation

$$p(t) = p_0 \frac{v(t - t_n)}{s(t)}, \tag{11}$$

where t_n is the moment of the previous break, and $p_0 = (u_x m c_0^2)|_{t=0}$ is the initial pressure in the rod, where $c_0 = \sqrt{r/m}$ is the ice sound velocity. Therefore, the ice rod breaks are determined by the relation

$$p(t_{n+1}) = p_0 \frac{v(t_{n+1} - t_n)}{s(t_{n+1})} = p_c. \tag{12}$$

We take the following boundary conditions for $u(x,t)$

$$u(q(t),t) = q(t) = w(0,t), \tag{13}$$

$$u(x,t) \to 0 \quad x \to +\infty. \tag{14}$$

The condition (13) is a contact relation between the ice rod and the beam, and the condition (14) is a radiation condition at infinity. The initial conditions for u are given by

$$u(x,0) = \phi_0(x), \quad u_t(x,0) = \phi_1(x), \quad x \in (q(0), \infty), \tag{15}$$

where $\phi_j(x)$ for $j = 1, 2$ are fast decreasing functions in x for $x \to \infty$ satisfying the compatibility conditions with (2), that is,

$$\phi_0(q(0)) = 0, \quad \phi_1(q(0)) = 0.$$

It is also assumed that

$$|\phi_j(x)| < c_j \exp(-b_j x), \quad b_j, c_j > 0, \tag{16}$$

where b_j, c_j are arbitrary constants.

Notice that the differential equations, boundary and initial conditions can be transformed to a dimensionless form when we rescale the variables. For the rescaling, the following relations are used: $\bar{x} = x/h$, $\bar{q} = q/h$, $\bar{s} = s/h$, $\bar{w} = w/h$, $\bar{u} = u/h$, $\bar{d_k} = d_k/h$, $c_0^2 = E/m$, $\bar{v} = v/c_0$, $\bar{t} = tc_0/h$, $\bar{\alpha} = \alpha/m_0 c_0 h^2$, $\bar{\beta} = h\beta/mc_0$, $\bar{D} = D/m_0(c_0 h)^2$, $\bar{k}_0 = k_0 h^2/mc_0^2$, $\bar{\delta_0} = \delta_0 c_0/h$, $\epsilon = k_0/c_0^2 F$.

It is obvious that the parameter ϵ is small. To simplify notations, we omit now the bars and obtain the equations:

$$Dw_{zzzz} + w_{tt} + \alpha w_t = \epsilon(u_x + \delta_0 u_{xt})\delta(z)|_{x=q(t)}, \tag{17}$$

where $z \in [-H_1, H_2]$, and

$$\begin{aligned} &u_{xx} - u_{tt} - \beta u_t - k_0 u + \delta_0 u_{xxt} \\ &\quad = -\beta s_t - k_0 s, \quad t > 0, \quad q(t) < x < \infty, \end{aligned} \tag{18}$$

where the initial conditions are

$$q(0) = 0, \quad q_t(0) = 0, \tag{19}$$

$$u(x, 0) = \phi_0(x), \quad u_t(x, 0) = \phi_1(x), \quad q(0) < x < \infty, \tag{20}$$

and where the boundary conditions for w and u are given by (3–5) and by (13), (14).

In the next sections we will approximate the solution of the initial-boundary value problem (17–20).

3 Galerkin decomposition for $w(z, t)$

As a first step, in solving the initial-boundary value problem (17–20) we apply a Galerkin decomposition for $w(x, t)$.

We seek the beam displacement $w(z, t)$ in the form as used in the standard Galerkin method:

$$w(z, t) = \sum_{n=1}^{\infty} W_n(t)\psi_n(z), \tag{21}$$

where $W_n(t)$ are unknown time-dependent coefficients and $\psi_n(z)$ are eigenfunctions of the corresponding spectral problem (see also Appendix 1):

$$\frac{d^4\psi_n}{dz^4} = \lambda_n \psi_n, \tag{22}$$

satisfying the boundary conditions

$$\psi_n(z)|_{z=-H_1} = \psi_{n_z}(z)|_{z=-H_1} = 0 \tag{23}$$

at the bottom, and

$$\psi_{n_{zz}}(z)|_{z=H_2} = \psi_{n_{zzz}}(z)|_{z=H_2} = 0 \tag{24}$$

at the top of the beam.

The linear operator (defined by those equations and boundary conditions) is self-adjoint. So, the eigenvalues λ_n are real and positive, and the corresponding eigenfunctions ψ_n are orthonormal. For the coefficients W_n one obtains from (17) the following system of ordinary differential equations:

$$\begin{aligned} &\frac{d^2 W_n(t)}{dt^2} + \alpha \frac{dW_n(t)}{dt} + \Omega_n^2 W_n \\ &\quad = \mu(W)\psi_n(0), \quad n = 1, 2, \ldots, \end{aligned} \tag{25}$$

where Ω_n are natural frequencies of the beam. Note that μ depends on the coefficients

$$W = (W_1, W_2, \ldots)$$

due to the boundary conditions at the beam-ice rod contact (see 5, 17), and therefore Eq. (25) can be considered as an infinite system of coupled oscillators. That coupling, as we will see in the next sections, leads to nonlinear effects and bifurcations.

4 Asymptotic solutions for the amplitude coefficients in $w(z, t)$

The asymptotic approach to study the system of equations (25) is well known, see [6,7]. Let $\tau = \epsilon t$ be a slow time. It is assumed that $\alpha = \epsilon\bar{\alpha}$, where $0 < \bar{\alpha} < C$, with C a positive constant independent of ϵ. Furthermore, it should be observed that the right-hand side of (17) is of order ϵ and depends on t and q. For that reason we look for solutions W_n of (17) in the form

$$W_n = W_{n,0}(t, \tau) + \epsilon W_{n,1}(t, \tau) + \ldots, \tag{26}$$

where

$$W_{n,0} = A_n(\tau)\sin(\Omega_n t + \phi_n(\tau)),$$

and where the amplitude A_n and the phase ϕ_n are unknown slowly time-varying functions. From (26) it follows that

$$\begin{aligned} \partial_t W_{n,0} = &(\Omega_n + \epsilon\phi_{n\tau})A_n(\tau)\cos(\Omega_n t + \phi_n(\tau)) \\ &+ \epsilon A_n(\tau)_\tau \sin(\Omega_n t + \phi_n(\tau)), \end{aligned}$$

and

$$\begin{aligned}\partial_{tt} W_{n,0} = & -\Omega_n^2 \cos(\Omega_n t + \phi_n(\tau)) \\ & + 2\epsilon\Omega_n (A_{n\tau} \cos(\Omega_n t + \phi_n(\tau)) \\ & - A_n \phi_{n\tau} \sin(\Omega_n t + \phi_n(\tau)) + O(\epsilon^2).\end{aligned}$$

By substituting these relations into (25), and by taking together terms of order ϵ, one obtains the following equation for $W_{n,1}$:

$$W_{n,1_{tt}} + \Omega_n^2 W_{n,1} = S_n(A, \phi, t, \epsilon), \tag{27}$$

where

$$\begin{aligned}S_n = 2\Omega_n \Big(& -A_{n\tau} \cos(\Omega_n t + \phi_n(\tau)) \\ & + A_n \phi_{n\tau} \sin(\Omega_n t + \phi_n(\tau)) \Big) + R_n(A, \phi, t),\end{aligned} \tag{28}$$

and

$$\begin{aligned}R_n(A, \phi, t) = & \mu(W(A, \phi))\psi_n(0) \\ & - \alpha\Omega_n A_n \cos(\Omega_n t + \phi_n(\tau)),\end{aligned} \tag{29}$$

and where $A = (A_1, A_2, \ldots)$ and $\phi = (\phi_1, \phi_2, \ldots)$ denote infinite sequences of the functions $A_n(\tau)$ and $\phi_n(\tau)$ with $n = 1, 2, ..,$ respectively. Let $\langle f \rangle$ denote the average of a continuous uniformly bounded function f:

$$\langle f \rangle = \lim_{T \to \infty} \int_0^T f(t) dt.$$

For large times $t = O(\epsilon^{-1})$ Eq. (27) has bounded solutions in t if and only if

$$\langle S_n(A, \phi, t, \epsilon) \cos(\Omega_n t + \phi_n) \rangle = 0, \tag{30}$$

and

$$\langle S_n(A, \phi, t, \epsilon) \sin(\Omega_n t + \phi_n) \rangle = 0. \tag{31}$$

Finally, it follows from (30) and (31) that the following system of equations for the amplitude A_n and the phase ϕ_n are obtained:

$$\Omega_n A_{n\tau} = \langle R_n(A, \phi, t) \cos(\Omega_n t + \phi_n) \rangle, \tag{32}$$

and

$$\Omega_n A_n \phi_{n\tau} = -\langle R_n(A, \phi, t) \sin(\Omega_n t + \phi_n) \rangle. \tag{33}$$

We investigate this system in the next section.

5 Asymptotic formulas for the ice rod displacement $u(x, t)$

The ice rod displacement is studied in detail in [2]. We repeat here the main formulas needed for the analysis of (32–33).

5.1 Assumptions

The aim of this subsection is to express the displacement $u(x, t)$ in q, and obtain an equation involving q only. We use the following assumption:

$$0 < \Omega_1 \ll k_0^{1/2}, \tag{34}$$

i.e., the first natural frequency of the beam is small with respect to the cut-off frequency of the ice rod. We also assume that all coefficients associated with friction and damping effects are small, i.e.,

$$0 < \beta, \quad \delta_0 \ll \Omega_1. \tag{35}$$

It is useful to introduce two other small parameters

$$\eta = \beta k_0^{-1/2} \ll 1, \quad \lambda = \Omega_1 k_0^{-1/2} \ll 1. \tag{36}$$

To find u we first define an auxiliary function $V(t)$ as a solution of the following second-order ODE:

$$V_{tt} + \beta V_t + k_0 V = \beta s_t + k_0 s. \tag{37}$$

We seek the solution u of (18) in the form $u = V(t) + \bar{u}$, where $\bar{u}$ satisfies the following equation,

$$\bar{u}_{xx} - \bar{u}_{tt} - \beta \bar{u}_t + \delta_0 \bar{u}_{xxt} - k_0 \bar{u} = 0, \tag{38}$$

and the boundary and initial conditions:

$$\bar{u}(q(t), t) = q(t) - V(t), \tag{39}$$

$$\lim_{x \to +\infty} \bar{u}(x, t) = -V(t), \tag{40}$$

$$\begin{aligned}\bar{u}(x, 0) = & \phi_0(x) - V(0), \\ \bar{u}_t(x, 0) = & \phi_1(x) - V'(0),\end{aligned} \tag{41}$$

where $V' = dV/dt$. In the next subsections we determine the auxiliary function V, and construct an asymptotic approximation for $\bar{u}$. To simplify the computations, let us assume that $d_n = d$. Then $s(t)$ is a periodic function with period $T = d/v$, and $\omega = 2\pi/T = 2\pi v/d$ is the breaking frequency of an ice rod. For the Fourier coefficients $\hat{s}_n$ of s one has

$$\hat{s}_n = \frac{id}{2\pi n} \quad (n \neq 0), \quad \hat{s}_0 = d/2. \tag{42}$$

The Fourier series for V has the form

$$V(t) = \sum_{n \in \mathbb{Z}} \hat{V}_n \exp(i\omega n t) + \tilde{V}(t), \tag{43}$$

where the function $\tilde{V}(t)$ is the homogeneous solution of (37) and decreases in t with an exponential rate, and the Fourier coefficients in (43) are defined by

$$\hat{V}_n = \frac{\hat{s}_n(k_0 + i\beta n\omega)}{k_0 - (n\omega)^2 + i\beta n\omega}, \quad n \neq 0. \tag{44}$$

The coefficient $\hat{V}_0 = d/2$ is the average of V. Note that the term $\tilde{V}(t)$ is exponentially decreasing in t and therefore we leave out that term for large times $t \gg \beta^{-1}$.

5.2 Asymptotics for $\bar{u}$

Let us introduce a new variable: $y = x - q(t)$. Then for $\bar{u}(x,t) = \tilde{u}(y,t)$ one has $\tilde{u} \approx \tilde{u}^{(0)} + \tilde{u}^{(1)}$, where the $\tilde{u}^{(k)}$ functions are defined as follows.

The complex frequencies $\hat{\omega}_n$ are defined by

$$\hat{\omega}_n^2 = k_0 + i\beta\omega n - n^2\omega^2 \tag{45}$$

and

$$\hat{\Omega}_n^2 = k_0 + i\beta\Omega_n - \Omega_n^2. \tag{46}$$

In (46), as usual, we choose the signs of the complex roots such that the negative real parts for $\hat{\omega}_n$ and $\hat{\Omega}_n$ are obtained. Then for $\Omega_n^2 \ll k_0$ one has

$$\hat{\Omega}_n \approx -{k_0}^{1/2} - i\frac{\beta\Omega_n}{2k_0^{1/2}}. \tag{47}$$

Following [2] we obtain

$$\tilde{u}^{(0)}(y,t) \approx \sum_{n=1}^{+\infty} W_n(t)\psi_n(0)\mathrm{Re}\exp(\hat{\Omega}_n y) - \sum_{n=1}^{+\infty} \hat{V}_n \exp(\bar{\omega}_n y + in\omega t), \tag{48}$$

where $\bar{\omega}_n = \hat{\omega}_n(1 + \delta_0 in\Omega_n)^{-1/2}$. In this relation, we represent the beam as a set of oscillators with frequencies close to $\hat{\Omega}_n$. The Fourier series in the right-hand side of (48) converges since $\hat{V}_n$ is $O(n^{-2})$ as $n \to \infty$. A natural approximation for $\tilde{u}^{(1)}$ is:

$$\tilde{u}^{(1)}(y,t) = G_1(y,t)q_t(t) + G_2(y,t)q_{tt}(t) + G_3(y,t)q_t^2(t) + O(\lambda),$$

where

$$G_1(y,t) = y\Big(G_{10}(y,t) + G_{11}q + G_{12}q_t\Big), \tag{49}$$

$$G_2(y,t) = y\Big(G_{20} + G_{21}q\Big), \tag{50}$$

$$G_3(y,t) = y\Big(G_{30} + G_{31}q\Big), \tag{51}$$

where

$$G_{10} = \sum_{n\in\mathbb{Z}} (in\omega + \beta/2 - \delta_0\bar{\omega}_n^2/2)\hat{V}_n \exp(\bar{\omega}_n y + i\omega nt), \tag{52}$$

$$G_{11} = -\frac{1}{2}(\beta - \delta_0\bar{\omega}^2)\mathrm{Re}\exp(\bar{\omega}y),$$

$$G_{12} = -\mathrm{Re}\exp(\bar{\omega}y), \tag{53}$$

$$G_{20} = \frac{1}{2}\sum_{n\in\mathbb{Z}} \hat{V}_n \exp(\bar{\omega}_n y + i\omega nt),$$

$$G_{21} = \frac{1}{2}\mathrm{Re}\exp(\bar{\omega}y), \tag{54}$$

$$G_{30} = -\frac{1}{2}\sum_{n\in\mathbb{Z}} \bar{\omega}_n\hat{V}_n \exp(\bar{\omega}_n y + i\omega nt), \tag{55}$$

$$G_{31} = \frac{1}{2}\mathrm{Re}\bar{\omega}\exp(\bar{\omega}y). \tag{56}$$

The relations (49–56) allow us to find the deformation at $x = q(t)$ and further to find the amplitude coefficients $W_n(t)$.

5.3 Ice floe deformation at the edge of the rod

The relations obtained in the previous subsections show that the deformation $\tilde{u}_y$ at $y = 0$ has the form

$$\tilde{u}_y(0,t) = S(t,q,q_t,q_{tt}), \tag{57}$$

where

$$S(t,q,q_t,q_{tt}) = \mathrm{Re}\bar{\omega}q + F_0(t) + F_1(t)q_t + F_2(t)q_{tt} + F_3(t)q_t^2 + F_4(t)qq_t + F_5(t)qq_{tt} + F_6(t)qq_t^2, \tag{58}$$

where

$$F_0(t) = -\sum_{n\in\mathbb{Z}} \bar{\omega}_n\hat{V}_n \exp(i\omega nt), \tag{59}$$

and

$$F_1 = G_{10}(y,t)|_{y=0}, \quad F_2 = G_{20}(y,t)|_{y=0},$$
$$F_3 = (G_{12} + G_{30})(y,t)|_{y=0}, \quad F_4 = G_{11}(y,t)|_{y=0},$$
$$F_5 = G_{21}(y,t)|_{y=0}, \quad F_6 = G_{31}(y,t)|_{y=0}.$$

For the coefficients $F_1, F_2, \ldots, F_6$ we obtain (see also (52–56))

$$F_1(t) = \sum_{n\in\mathbb{Z}} \Big(in\omega + \frac{\beta}{2} - \frac{\delta_0\bar{\omega}_n^2}{2}\Big)\hat{V}_n \exp(i\omega nt), \quad (60)$$

$$F_2(t) = \frac{1}{2}\sum_{n\in\mathbb{Z}} \hat{V}_n \exp(i\omega nt), \quad (61)$$

and

$$F_3(t) = -1 - \frac{1}{2}\sum_{n\in\mathbb{Z}} \bar{\omega}_n \hat{V}_n \exp(i\omega nt), \quad (62)$$

$$F_4 = -\frac{\beta - \delta_0 \mathrm{Re}\bar{\omega}^2}{2},$$

$$F_5 = -1/2, \quad F_6 = \frac{\mathrm{Re}\bar{\omega}}{2}. \quad (63)$$

In the next section the ODE for $q(t)$ will be studied by using the averaging method as presented in Sect. 4 of this paper.

6 The nonlinear equations for the amplitude functions $A_n(t)$ in $w(z, t)$

6.1 Equations for the amplitudes A_n and the phases ϕ_n

In contrast to [1] we are dealing here with many A_n functions. Note that

$$q(t) = \sum_{n=1}^{\infty} W_n(t)\psi_n(0). \quad (64)$$

The coefficients W_n can be represented by asymptotic series, and it follows from Sect. 4 of this paper that the function $q(t)$ can be approximated by

$$q(t) = \sum_{n=1}^{\infty} \psi_n(0) A_n(\tau)\sin(\Omega_n t + \phi_n(\tau)), \quad (65)$$

where $A_n(\tau)$ and $\phi_n(\tau)$ satisfy (32) and (33), respectively. To approximate $A_n(t)$ and $\phi_n(t)$ we introduce the auxiliary function

$$R_n(t, \tau) = \cos(\Omega_n t + \phi_n(\tau)) + \delta_0\Omega_n \sin(\Omega_n t + \phi_n(\tau)).$$

From Sect. 4 it follows that the coefficients $A_n(\tau)$ slowly evolve in time according to the following equation:

$$\begin{aligned}\Omega_n \frac{dA_n}{d\tau} &= D_n(v, \phi) + D_{1,n}(v, \phi, A)\\ &\quad + D_{2,n}(v, \phi, A) + D_{3,n}(v, \phi, A)\\ &\equiv P_n(v, \phi, A), \end{aligned} \quad (66)$$

where $D_{1,n}(v, A, \phi)$, $D_{2,n}(v, A, \phi)$ and $D_{3,n}(v, A, \phi)$ are linear, bilinear, and trilinear operators, respectively, while D_n is independent of A. These operators and D_n can be found as follows. By integrating by parts, and by using expression (58) we obtain

$$D_n(v, \phi) = \langle F_0(t) R_n(t, \tau)\rangle, \quad (67)$$

$$D_{1,n}(v, \phi, A) = \langle(\mathrm{Re}\bar{\omega}\, q + (F_1(t) - \alpha\lambda_n)q_t \quad (68)$$

$$+F_2(t)q_{tt})R_n(t, \tau)\rangle, \quad (69)$$

$$D_{2,n}(v, \phi, A) = \langle(F_3 q_t^2 + F_4 q q_t + F_5 q q_{tt})$$

$$R_n(t, \tau)\rangle, \quad (70)$$

$$D_{3,n}(v, \phi, A) = \langle F_6 q q_t^2 R_n(t, \tau)\rangle. \quad (71)$$

By substituting the expression (65) for $q(t)$ into (68) one obtains

$$D_{1,n}(v, \phi, A) = \sum_{n_1=1}^{\infty} d^{(1)}_{nn_1} A_{n_1}, \quad (72)$$

where

$$d^{(1)}_{nn_1} = \psi_{n_1}(0)\Big(\langle R_{nn_1}(t) R_n(t, \tau)\rangle - \alpha\lambda_n\delta_{nn_1}\Big),$$

where

$$\begin{aligned} R_{nn_1} &= \big(\mathrm{Re}\bar{\omega} - F_2(t)\Omega_{n_1}^2\big)\sin(\Omega_{n_1}t + \phi_{n_1})\\ &\quad + F_1(t)\Omega_{n_1}\cos(\Omega_{n_1}t + \phi_{n_1}), \end{aligned}$$

and where δ_{nm} stands for the Kronecker symbol, $\delta_{nm} = 1$ for $n = m$, otherwise $\delta_{nm} = 0$. Similarly, from (70) and (68) it follows that

$$D_{2,n}(\phi, v, A) = \sum_{n_1=1}^{\infty}\sum_{n_2=1}^{\infty} d^{(2)}_{nn_1n_2} A_{n_1} A_{n_2}, \quad (73)$$

where

$$\begin{aligned} &d^{(2)}_{nn_1n_2}\\ &= \psi_{n_1}(0)\psi_{n_2}(0)\Big\langle\Big(F_3\Omega_{n_1}\Omega_{n_2}\cos(\Omega_{n_1}t + \phi_{n_1})\\ &\quad\times\cos(\Omega_{n_2}t + \phi_{n_2}) + F_4\Omega_{n_2}\sin(\Omega_{n_1}t + \phi_{n_1})\\ &\quad\times\cos(\Omega_{n_2}t + \phi_{n_2}) - F_5\Omega_n^2\sin(\Omega_{n_1}t + \phi_{n_1})\\ &\quad\times\sin(\Omega_{n_2}t + \phi_{n_2})\Big)R_n(t, \tau)\Big\rangle, \end{aligned}$$

and from (71) and (68) it follows that

$$\begin{aligned} &D_{3,n}(v, \phi, A)\\ &= \sum_{n_1=1}^{\infty}\sum_{n_2=1}^{\infty}\sum_{n_3=1}^{\infty} d^{(3)}_{nn_1n_2n_3} A_{n_1} A_{n_2} A_{n_3}, \end{aligned} \quad (74)$$

where

$$d^{(3)}_{nn_1n_2n_3} = \psi_{n_1}(0)\psi_{n_2}(0)\psi_{n_3}(0)F_6\Omega_{n_2}\Omega_{n_3} \times \langle \sin(\Omega_{n_1}t + \phi_{n_1})\cos(\Omega_{n_2}t + \phi_{n_2}) \times \cos(\Omega_{n_3}t + \phi_{n_3})R_n(t,\tau)\rangle.$$

For the phase ϕ_n it follows from (33) and (68) that an equation similar to (66) can be obtained, that is,

$$\Omega_n A_n \frac{d\phi_n}{d\tau} = \Phi_n(v, A, \phi) \tag{75}$$

involving linear, quadratic and cubic terms. In the coming subsection we will find asymptotics for $P_n(v, \phi, A)$. These computations show that $P_n(v, \phi, A)$ does not depend on the phase ϕ. Therefore, Eqs. (66) and (75) can be solved separately. As a first step we find the amplitudes A_n from (66), and then we can find the phase ϕ_n from (75).

6.2 Large time behaviour of the solutions $A_n(\tau)$ of equation (66)

We suppose that there are m and n such that

$$m\omega \approx 2\Omega_n \tag{76}$$

but there are no m and n such that

$$m\omega \approx 3\Omega_n, \quad m\omega \approx \Omega_n. \tag{77}$$

Then under the assumptions (76) and (77) it is easy to check that $D_n(v) \equiv 0$ and $D_{2,n}(v, \phi, A) \equiv 0$. For $D_{3,n}(v, \phi, A)$ it follows from (74) that:

$$D_{3,n}(v, \phi, A) = -\bar{C}A_n \sum_m |\Omega_m|^2 |A_m|^2,$$

where $\bar{C} = \delta \mathrm{Re}\bar{\omega} < 0$. Taking into account these relations and (72) it follows that Eq. (66) reduces to

$$\Omega_n \frac{dA_n}{d\tau} = \sum_m d^{(1)}_{nm} A_m - A_n \bar{C} Z, \tag{78}$$

where

$$Z = \sum_m |\Omega_m|^2 |A_m|^2$$

is an asymptotic approximation of the kinetic energy of the beam. By using the nonlinear Eq. (78), we are able to estimate solutions and to check the existence of pitchfork bifurcations. This analysis is standard and long, but quite straightforward, and it is presented in Appendix 2 and in Appendix 3. Here, we formulate the main results and their physical and mechanical interpretation.

Result I: Solutions of system (78) tend to equilibrium solutions A^{eq} for $\tau \gg 1$.

Result II: Let us consider the polynomial $P_1(v)$, defined by

$$P_1(v) = -\alpha - c_1 m^3 v^{-2} + c_2 v^{-1}, \tag{79}$$

where $v \in (0, \infty)$ is the ice rod speed, and c_i are positive constants, which depend on the problem parameters but are independent of v. If this polynomial takes a positive maximum value for a certain v_*, then there exist two bifurcations. Let $V_+ = (v_1, v_2)$ be the interval, where $P_1(v)$ takes positive values (which are bounded). For $v \notin V_+$ one has

$$A^{eq}_n \approx O(\epsilon),$$

while for $v \in V_+$ one has equilibrium solutions defined by

$$|A^{eq}_n| \approx C\ P_1(v)^{1/2}, \quad C > 0, \quad n \in \mathrm{Res}(1),$$
$$|A^{eq}_n| = O(\epsilon), \quad n \notin \mathrm{Res}(1),$$

where $\mathrm{Res}(1)$ is a finite subset of indices n, $\mathrm{Res}(1) \subset \mathbb{N}$. The number of equilibrium solutions is 2^M, where $M = \mathrm{Res}(1)$ is the number of elements in the set $\mathrm{Res}(1)$ (the set of possible resonances causing the largest amplitudes).

The mathematical proofs of these results can be found in Appendix 2 and Appendix 3. Let us discuss their non-formal interpretations.

Two approaches were developed to explain ice induced vibrations. The first one is based on the idea of resonance between an elastic structure and periodic breaking of an ice rod at a frequency ω. According to an alternative approach the cause of ice induced vibration is the self-excited oscillation due to a negative friction.

Our approach (which uses a beam model) connects both approaches. Namely, a resonance between the ice breaking and the structure can lead to a negative friction. It can be described by a polynomial P_1 (see Eq. 99). In this polynomial the first term represents the usual internal structure friction (with a minus sign). The second term and the third term in P_1 are contributions of the ice-structure interaction. The sum of all terms can be positive, if α is not too large. Positive values of P_1 correspond to negative effective friction.

What can occur when $P_1(v)$ is positive ? To understand this we consider the sets $\mathrm{Res}(m)$ consisting of indices n which correspond to resonance modes ψ_n,

where $m\omega \approx \Omega_n$ (in which ω is the frequency of the periodic ice breaking, and Ω_n is the n-th frequency of the free oscillation of the structure). The main resonance effect first arises when $m = 1$, and moreover, it is the strongest resonance (with respect to $m = 2, \ldots$). The instability of the structure occurs at the first natural frequency of the beam. To simplify the statement let us consider the case when we are dealing with a single resonance mode only, i.e., $M = 1$. Then, we see from (84) that our equation for the equilibrium amplitude A_1 reads (the small contributions of the order $O(\epsilon)$ terms are neglected)

$$g(v)P_1(v)A_1 - A_1^3 = 0, \tag{80}$$

where $g(v)$ is a positive function depending on the ice rod speed v. Although Eq. (80) is simple, it is fundamental in physics, where it occurs in the theory of the second phase transitions developed by L. Landau. Mathematically this Eq. (80) describes a pitchfork bifurcation. For negative P_1 we have a trivial solution $A_1 = 0$ while for $P_1(v) > 0$ there exist two solutions $A_1 = \pm\sqrt{g(v)P_1(v)}$. Actually in our problem we observe two pitchfork bifurcations, a direct one, leading to the instability onset at $v = v_1$, and an inverse one, which produces damping for large oscillations (see Fig. 3).

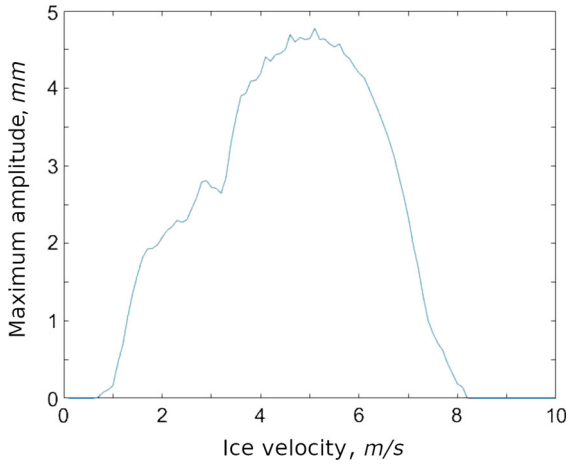

Fig. 3 Dependence of the average magnitude $\|A\|$ on the speed v. The dimensionless parameter values are : the friction $\alpha = 0.01$, $\delta = 0.1$, $\beta = 1$, $\kappa = 0.1$, $k_0 = 0.1$. The number of beam modes which are taken into account is $M = 60$

6.3 Main results

In Fig. 3, which is obtained by using the analytical equations and numerical simulations, we see the following main effects:

(i) instability at a certain speed v leading to a sharp amplitude increase;
(ii) then a growth of the amplitude $\|A\|$;
(iii) breakdown to a small amplitude at a second critical speed.

We observe here a plateau, and the results in Fig. 3 are consistent, at least qualitatively,with the results as obtained in [22,29].

7 Discussion and conclusions

In this paper an interaction between an elastic structure and an ice floe is studied by using a new analytical approach. The analytical results describe to a great extent the dynamic behavior of the beam. The verification of the obtained asymptotic approximations of the solution is performed in the same way as in [2], and shows a good agreement with the numerical solution of the system of equations describing the problem at times of order $1/\epsilon$. The results are also compared with some current IIV models. The system parameters necessary for the calculations are chosen in the following way. The bulk viscosity is the same as in [2] using data which can be found in [24,26,27,34]. The calculations reveal that if we take $\delta_0 = 3 \cdot 10^9$ Pa·s and $\beta = 0.75 \cdot 10^9$ Pa·s, then the obtained results are in good agreement with the results as obtained by using other IIV models and experimental data. Such parameters as the length and bending rigidity of the beam were taken depending on the IIV model to which the beam model was compared. The generalized rigidity and mass of the beam should be equal to the rigidity and mass of the oscillator, respectively. This can be accomplished by using the Rayleigh method. In Fig. 4a the proposed model results are presented for the continuous brittle crushing regime at 0,02 m/sec. If we compare these results with the experimental data from [36] (see Fig. 4b) we can find a good agreement in time behavior and in values for the maximum of the oscillation amplitude. In Fig. 5 Curve 1 depicts the beam displacements in the lock-in regime at 0.18 msec^{-1} as obtained by the model presented in this paper, and Curve 2 gives the model results from

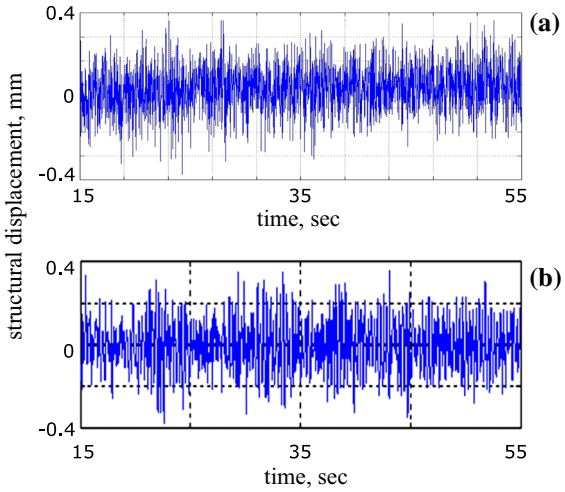

Fig. 4 The dependence of the displacement on time during continuous brittle crushing regime at a velocity of 0.02 msec^{-1}

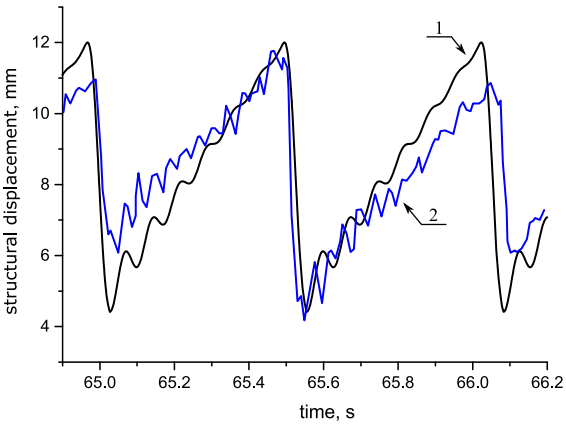

Fig. 5 The dependence of the displacement on time during an intermittent crushing at a velocity of 0.13 msec^{-1}. Comparison displacements as obtained in this paper (Curve 1) with the displacements as obtained in [36] (Curve 2)

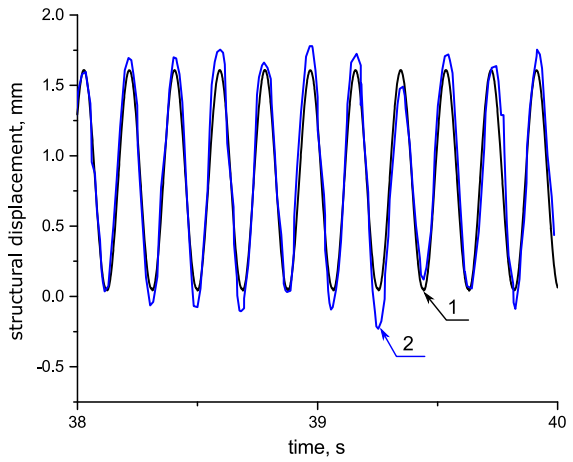

Fig. 6 The dependence of the displacement on time during frequency lock-in at an indention speed of 0,18 msec^{-1} (Curve 1: model results as obtained in this paper; Curve 2: experimental data from [28]

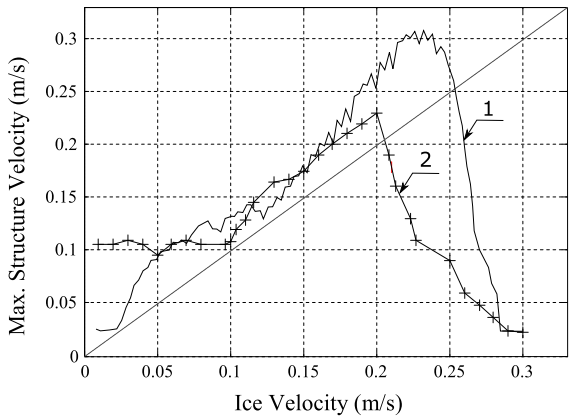

Fig. 7 The dependence of the maximal structural velocity on the ice velocity during the steady-state vibration. Comparison of the results as obtained in this paper (Curve 1) to those as obtained in [15] (Curve 2)

[28]. In Fig. 6 Curve 1 describes the displacements as obtained by using the model proposed in this paper for the intermittent crushing at 0.13 msec^{-1}; This curve has the order of displacements for the same regimes, as obtained by using the model proposed in [13,36]. In Fig. 7 Curve 1 depicts the maximal structural velocities during the steady-state vibration as obtained by the model as described in this paper, and Curve 2 , the ones as obtained in [15]. Also these results show a good match with the results as obtained in [17].The differences at the down branches in Fig. 7 are due to the fact that the values of the beam damping coefficient and the ice friction coefficients as used in this paper may be different from those which were used by the author of [15] in the test (unfortunately, the author of [15] did not provide the data for those parameters).

The real structure is of course a 3D object for which the spectrum of natural frequencies can be located densely, and vibrations may occur not only in one plane. Those features of the structure will be taken into account in future research. In 2D beam models the fact that eigenvalues of the operator-spectrum , which describe the structure, can be dense, was partly used in the analysis as presented in this paper.

The main obtained results are:

(I) For beams, perturbed by small nonlinearities and a small damping, the concept of quasi-mode is introduced. The quasi-mode is a linear combination of the usual eigenmodes. The large time behaviour of solutions at the instability onset is determined by a single quasi-mode, which is maximally linearly unstable.

(II) As we mentioned in the introduction two theories compete to explain the ice induced vibrations of structures which interact with a moving ice floe. Our analysis shows that, in a sense, both theories are correct. The instability exists, and it is generated by a force leading to nonlinear resonances of the beam. An instability arises as follows. The resonance caused by regular breaking of the ice rod at particular values of the ice rod speed lead to a change of sign of the polynomial P_1, and creates an effective negative friction. As a result, the beam vibrations grow but the amplitudes are bounded due to the nonlinear terms which are also generated by the interaction between the beam and the ice rod. Vibration amplitudes can be computed by a quasi-mode approach, and we show that the mean square of the beam displacement is proportional to the number of resonance modes.

Author contributions AKA: Conceptualization, Methodology, Formal analysis. SAV: Methodology, Formal analysis. WTH: Conceptualization, Validation.

Data availability The data that support the findings of this study are available from the corresponding author, upon reasonable request.

Appendix 1: Eigenfunctions of the beam operator

The eigenfunctions $\psi_n(z)$ can be found as follows. Consider the problem where the functions ψ_n satisfy the differential equation:

$$d^4\psi_n/dz^4 = \lambda_n\psi_n, \quad -H_1 < z < H_2 \tag{81}$$

and the boundary conditions

$$\psi_n(z)|_{z=-H_1} = \psi_{n_z}(z)|_{z=-H_1} = 0, \tag{82}$$

$$\psi_{n_z}(z)|_{z=H_2} = \psi_{n_{zz}}(z)|_{z=H_2} = 0. \tag{83}$$

The operator d^4/dz^4 is self-adjoint under the boundary conditions (82) and (83). By multiplying both sides of Eq. (81) by ψ_n and by integrating by parts one obtains that $\int_{-H_1}^{H_2}(d^2\psi/dz^2)^2 = \lambda_n\int_{-H_1}^{H_2}\psi^2$ thus $\lambda_n > 0$. Let $k = \lambda_n^{1/4} > 0$. The roots $k^4 = \lambda_n$ have the form $k_1 = k$, $k_2 = -k$, $k_3 = \sqrt{-1}k$ and $k_4 = -\sqrt{-1}k$. Therefore, the eigenfunctions ψ_n can be represented as follows:

$$\psi_n(z) = C_1\cosh(k(z+H_1)) + C_2\sinh(k(z+H_1)) + C_3\cos(k(z+H_1)) + C_4\sin(k(z+H_1)).$$

By using the boundary conditions (82) we obtain that $C_2 = -C_4$ and $C_1 = -C_3$, and by using the boundary conditions (83) one finally obtains that $detA(k) = 0$, where A is a square 2×2 matrix with entries

$$a_{11} = \sinh(k\Delta H) + \sin(k\Delta H),$$
$$a_{12} = \cosh(k\Delta H) + \cos(k\Delta H),$$
$$a_{21} = \cosh(k\Delta H) + \cos(k\Delta H),$$
$$a_{22} = \sinh(k\Delta H) - \sin(k\Delta H),$$

where $\Delta H = H_2 + H_1$ is the length of the beam. Then a straightforward computation gives an equation for k:

$$\cosh(k\Delta H)\cos(k\Delta H) = 1.$$

For large k (which corresponds to large n) we have $k\Delta H \approx \pi/2 + n\pi$. The eigenfunctions form a complete orthonormal basis in the space $L_2[H_1, H_2]$. The key observation is that since the beam (platform) is a macroscopic object, with large sizes, the spectrum of the beam-oscillations can be dense and the eigenvalues can be located densely.

Appendix 2: Investigation of the nonlinear equation (78)

To investigate system (78), let us change the variable $A_n = X_n/\Omega_n$ and let us denote $B_{nm} = \Omega_m^{-1}d_{nm}^{(1)}$. Then, for the new unknown X_n one has

$$\frac{dX_n}{d\tau} = \sum_{m=1,2,\ldots} B_{nm}X_m - \bar{C}ZX_n, \tag{84}$$

where

$$Z = \sum_m |X_m|^2. \tag{85}$$

The approach, followed here, is similar to the famous theory of hypercycles developed to describe chemical and pre-biological evolution [31], but in our case we are dealing with another nonlinear form. Let us define

the Hilbert space $\mathbb{H}$ of sequences $\{X_n\}$, $n = 1, 2, \ldots$, with bounded norm $\|X\|$ defined by:

$$\|X\|^2 = \sum_{n=1}^{\infty} |X_n|^2.$$

The space $\mathbb{H}$ has a clear mechanical interpretation: it is the set of all beam states with a bounded kinetic energy. Let θ^l be eigenfunctions of the operator $\mathbf{B}$ defined by the matrix with entries B_{nm} in the space $\mathbb{H}$ by $(\mathbf{B}X)_n = \sum_{m=1}^{\infty} B_{nm} X_m$. One can show that $\mathbf{B}$ is a compact operator in $\mathbb{H}$, thus $\mathbf{B}$ has a complete system of eigenfunctions and a countable set of eigenvalues λ_m (which can have any sign). Note that in numerical simulations, we truncate the possible values of m, where $m = 1, 2, \ldots$ at a certain level $m < N_{mode}$, and then the space $\mathbb{H}$ becomes a finite dimensional Euclidean space with standard norm. Therefore, in this case the compactness of $\mathbf{B}$ is obvious. We can represent X by the eigenvectors $\theta^{(m)}$ of the operator $\mathbf{B}$ in the following way:

$$X_n(\tau) = \sum_{m=1}^{\infty} \theta_n^{(m)} Y_m(\tau).$$

The vectors $Y = (Y_1, Y_2, \ldots, Y_m, \ldots)$ are called quasi-modes [31]. The quasi-modes are linear combinations of the usual modes X. Note that the matrix $\mathbf{B}$ is symmetric. Then there is an orthogonal transformation $\mathbf{U}$ such that the substitution $Y = \mathbf{U}X$ transforms $\mathbf{B}$ to a diagonal matrix, which has the same eigenvalues as $\mathbf{B}$. Moreover, the orthogonality property implies that this transformation conserves the norm, and thus $Z = \sum_{n=1}^{\infty} |Y_n^2|$.

Then, as a result of this transformation, Eq. (84) leads to the following system for the unknown coefficients Y_n:

$$\frac{dY_n}{d\tau} = \lambda_n Y_n - Y_n \bar{C} Z(\tau). \tag{86}$$

Assuming that the function $Z(t)$ is given, we obtain

$$Y_n(\tau) = Y_n(0) \exp\left(\lambda_n \tau - \bar{C} \int_0^{\tau} Z(s) ds\right). \tag{87}$$

Let us note that according to (85)

$$Z = \sum_m |Y_m|^2, \tag{88}$$

because the transformation $X \to Y$ conserves the norm $\| \|$. Substituting (87) into (88) we obtain the following equation for Z:

$$Z(\tau) \exp\left(2\bar{C} \int_0^{\tau} Z(s) ds\right) = h(\tau), \tag{89}$$

where

$$h(\tau) = \sum_n Y_n(0)^2 \exp(2\lambda_n \tau) > 0.$$

Equation (89) can be solved, yielding:

$$Z(\tau) = \frac{h(\tau)}{1 + 2\bar{C} \int_0^{\tau} h(s) ds}. \tag{90}$$

By substituting (90) into (87) one finally obtains

$$Y_n(\tau) = Y_n(0)\left(1 + 2\bar{C} \int_0^{\tau} h(s) ds\right) \exp(\lambda_n \tau). \tag{91}$$

This solution describes a competition between quasi modes Y_n ([31]). Finally in the limit $\tau \to \infty$ the main contribution in the beam displacement is given by a quasi-mode with the maximal $\mathrm{Re}\lambda_n = \mathrm{Re}\lambda_*$. Thus we obtain that

$$Y_*(\tau) \approx const \mathrm{Re}\lambda_*^{1/2} \quad \tau \gg 1 \tag{92}$$

$$|Y_n(\tau)| \ll |Y_*(\tau)|, \quad n > 1, \quad \tau \gg 1$$

for $\mathrm{Re}\lambda_* > 0$, and

$$Y_n(\tau) \approx O(\epsilon) \quad n > 1, \quad \tau \gg 1. \tag{93}$$

So, in the linear instability zone the large time behaviour of solutions of Eq. (84) is completely defined by the most unstable quasi-mode Y_*, which corresponds to $\lambda_* = \lambda_*(v)$. We will investigate that critical quantity $\lambda_*(v)$ in the next Appendix 3. It is important to note that all solutions $Y(t)$ (and therefore all solutions $A(\tau)$, which are linear combinations of Y_n) converge to an equilibrium solution. Moreover, although only a single quasi-mode Y_n determines the large time behaviour, we have a number of nonzero coefficients X_n (and thus A_n).

Appendix 3: Bifurcation analysis for (84)

Existence of bifurcations

We can show the existence of bifurcations for the dynamical system defined by (84) in two ways. The first one is as follows. We multiply the n-th equation in (84) by X_n^*, where the star denotes the complex conjugate of X_n. Summing up over all so-obtained equations, yields

$$\frac{dZ}{d\tau} = Q(v, X) - \bar{C} Z^2, \tag{94}$$

where

$$Q(v, X) = \sum_{m,n} B_{nm} X_m X_n.$$

The form Q can be estimated numerically and analytically. For small speeds v the quadratic form $Q(v, X)$ is negatively defined, because the friction term dominates:

$$Q(v, X) \le -c\|X\|^2, \quad c > 0.$$

where c is a constant. Then by (94) we obtain

$$\|X(\tau)\| \to 0 \quad (\tau \to +\infty).$$

On the other hand, for larger speeds the quadratic form $Q(X)$ is positively defined:

$$Q(v, X) \ge c_1\|X\|^2, \quad c_1 > 0.$$

where c_1 is a constant. Then by (94) we obtain

$$\|X(\tau)\| > \bar{X}_0 > 0 \quad (\tau \to +\infty).$$

So, we observe here the transition from trivial solutions to non-trivial solutions. Eq. (84) can be studied numerically. The results can be seen in Fig. 3.

Now we discuss an analytical approach, which allows us to obtain more precise information on eigenfunctions. Instability onset at a speed level v_c can be found by an analysis of the spectrum of the linear operator, which is defined by the linear term D_1. To correctly define that linear operator, we first introduce the space $\mathbf{H}_A$ of infinite sequences $A = (A_1, \ldots, A_n, \ldots)$. That space is defined by $\mathbf{H}_A = \{A : \|A\|^2 < \infty\}$ and it is equipped with the standard norm $\|A\| = \sqrt{\sum_{n=1}^{\infty} |A_n|^2}$. Let $\mathbf{D}^{(1)}(v)$ be the linear operator defined on $\mathbf{H}$ by

$$\mathbf{D}^{(1)}(v) = \sum_{n_1} d^{(1)}_{n,n_1} A_{n_1}.$$

Let us denote by $\lambda_*(v)$ the eigenvalue of this operator with the largest real part. Note that this quantity (as well as the operator itself) depends on the ice rod speed v. Then the instability onset (a bifurcation) arises if at a critical speed v_c one has

$$\mathrm{Re}\lambda_*(v_c) = 0, \text{ and } \mathrm{Re}\lambda_*(v) > 0 \quad \text{for } v > v_c. \quad (95)$$

One can show that there is an interval $I_{inst} = [v_c, v_s]$ for the speeds v such that

$$\mathrm{Re}\lambda_*(v) > 0, \quad v \in I_{inst}. \quad (96)$$

This can be shown in the following way. Let us compute first the entries $d^{(1)}_{n,n_1}$. For simplicity we suppose that $\delta_0 > 0$ is a small parameter and therefore we neglect the terms with δ_0 in the equation for R_n. Let us introduce the quantities $m_\pm(n, n_1)$ by the resonance conditions

$$|m_\pm(n, n_1)\omega - \Omega_n \pm \Omega_{n_1}| < \kappa \ll 1, \quad (97)$$

where $\kappa > 0$ is a small detuning parameter. These conditions (97) correspond to resonances between the ice rod breaking frequency and the natural frequencies of the beam. Then, we obtain

$$d^{(1)}_{n,n_1} = \Big(-\alpha\Omega_{n_1} + \frac{i}{2}\mathrm{Re}\hat{\Omega}_n\Big)\delta_{nn_1} + S_+(n, n_1) + S_-(n, n_1), \quad (98)$$

where

$$S_\pm(n, n_1) = \frac{\hat{\Omega}_{n_1}\hat{V}_{m_\pm}}{2} \times\big(-\sqrt{-1}\hat{\Omega}_{n_1} + (\sqrt{-1}m_\pm\omega + \beta/2)\big)$$

if there is a $m_\pm$ satisfying (97) with the corresponding sign, otherwise $S_\pm(n, n_1) = 0$. By using (98) one can show that the plot of $\mathrm{Re}\lambda^*(v)$ as a function of v can have a positive peak for some values of v. To see this, first let us note that $v \propto \omega$, and then consider the case for small $k_0 \ll m\omega$ and $\beta \ll k_0$. Then, we can use the following asymptotic approximation for $\hat{V}_m$:

$$\hat{V}_m \approx -\frac{idk_0}{2\pi m^3\omega^2}.$$

Substituting this formula into $d^{(1)}_{n,n_1}$ we obtain that these entries are defined by quadratic polynomials in $z = \omega^{-1} = const/v$, which have peaks at some $z = z_*$. These polynomials have the form

$$P_m(v) = -\alpha - \bar{c_1}m^3v^{-2} + \bar{c_2}v^{-1}, \quad (99)$$

where $\bar{c_1}$ and $\bar{c_2}$ some constants which are independent on v. For $d^{(1)}_{nn_1}$ one has

$$d^{(1)}_{nn_1} \approx \sum_m P_m(v)\delta_\kappa(m\omega(v) - \Omega_n - \Omega_{n_1}), \quad (100)$$

where δ_κ is an approximation of the δ-function by taking into account the conditions (97), where $\kappa > 0$ is a detuning parameter. The eigenvalues $\lambda^*(v)$ of the operator $\mathbf{D}^{(1)}(v)$ can be estimated by using the Rayleigh principle for the maximum of quadratic forms:

$$\lambda^*(v) = \max_{A,\, 0<\|A\|^2<\infty} Q(v, A), \quad (101)$$

where

$$Q(v, A) = \frac{\langle\mathbf{D}^{(1)}(v)A, A\rangle}{\|A\|^2}.$$

In this formula for Q the numerator is a sum of contributions of dissipation and effects caused by an interaction between the ice-rod and the beam. The denominator is the squared average over all modes of the beam displacement, i.e., $\|u\|^2$. By (100), the quadratic form can be estimated. In fact, we see that

$$Q(v, A) \approx \sum_m P_m(v) \sum_{n,n_1 \in \mathrm{Res}(m)} A_n A_{n_1}$$

under the condition that $\sum_n |A_n|^2 = 1$. Here $\mathrm{Res}(m)$ denotes the m-th set of resonances defined by the condition

$$\mathrm{Res}(m) = \{n, n_1 : \Omega_n + \Omega_{n_1} \in [m\omega - \kappa, m\omega + \kappa]\}.$$

The function $P_m(v)$ is fast decreasing in m, and we can take into account only the largest (first) term with $m = 1$, and then obtain

$$Q(v, A) \approx P_1(v) \sum_{n,n_1 \in \mathrm{Res}(m)} A_n A_{n_1}.$$

Assume that we take into account a finite set of modes, and that the number of elements (resonances) in the set Res(1) is bounded. Then, one can show that the optimal test vector A with a bounded norm is $A = (1/N_{res}, 1/N_{res}, \ldots, 1/N_{res}, 0, \ldots, 0, \ldots)$, where $1/N_{res}$ stands for the first N_{res} positions, and $N_{res}(v)$ is the number of resonances in the set Res(1) which depends on ω (and thus on v). As a result, we have a simple formula:

$$\lambda_*(v) = N_{res}(v) P_1(v). \tag{102}$$

Due to the special structure of our quadratic form Q, in the resonance case one has

$$A_n^{eq} \approx P_1(v)^{1/2}, \quad n \in \mathrm{Res}(1), \tag{103}$$

$$A_n^{eq} \approx O(\epsilon) \quad n \notin \mathrm{Res}(1), \tag{104}$$

for $P_1(v) > 0$, and

$$A_n^{eq} \approx O(\epsilon) \tag{105}$$

otherwise. Note that $\lambda_*(v)$ is negative for small v, because the negative term $-\bar{c_1} v^{-2} < 0$ dominates in $P_1(v)$. This means that contact interaction induces a positive damping. On the other hand, for very large v the terms $-\bar{c_1} v^{-2} < 0$ and $-\alpha$ dominate with respect to a positive contribution $\bar{c_2} v^{-1}$. This means that both for small and large velocities $\lambda_*(v) < 0$, the friction (damping) is positive and the solution has a small amplitude. These arguments explain the effects **(i)** and **(ii)** of Sect. 6.3. The sharp growth of the amplitude is a consequence of the fact that there are no resonances for small v and $N_{res}(v) = 0$. However, for some values v it is possible that $P_1(v) > 0$ and $\delta_\kappa(\omega(v) - \Omega_n - \Omega_{n_1}) \neq 0$. For such values the contact interaction generates a negative friction that creates a plateau as can be observed in Fig. 3. It is important to note that in the beam model that plateau extends the results with respect to the one degree of freedom oscillator model, because we have a number of modes with close frequencies Ω_n (the beam is a macroscopic object of large size). The number of resonances can be estimated. One can show that this number is a piecewise linear function of v (or ω). In fact, the number N_{res} is proportional to the area of the planar domain $\Omega_{\kappa,v}$ defined by

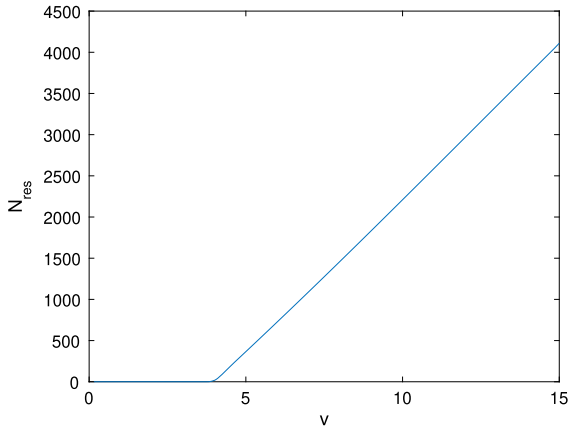

Fig. 8 This plot shows a typical dependence of $N_{res}(v)$. Here $\kappa = 0.3$, the velocity v lies in the interval $[0, 15]$ and Ω_n are uniformly distributed in the interval $[3, 10]$ with the step-size 0.07

$$\Omega_{\kappa,v} = \{(x, y) : x, y > a, |x + y - \omega| < \kappa\},$$
$$\omega = const \cdot v,$$

where $a = \min \Omega_n$. It is obvious that this area equals or tends to zero for small v and increases as a linear function of v for large v. A typical plot of $N_{res}(v)$ can be obtained by simulations as is shown in Fig. 8.

In order to proceed with a numerical analysis, we truncate the Galerkin series at some $n = M \gg 1$. Since the Fourier coefficients $\hat{V}_m$ are decreasing as $O(m^{-3})$, all series converge, and so this procedure can be justified. Let us compute two important quantities: $\bar{u}$ and $v_{b,\max}$. The first, $\bar{u}$ is the average of the mean square beam displacement with respect to time t, and is defined

as follows :

$$\bar{u} = T^{-1} \int_0^T \|u(\cdot, t)\| dt,$$

$$\|u(\cdot, t)\|^2 = \int_{-H_1}^{H_2} u(z, t)^2 dz,$$

where $T \gg 1$. This quantity is a natural measure for the beam displacement amplitude, however, it is hard to measure $\bar{u}$ in experiments. The quantity $v_{b,\max}$ is the maximal velocity of the beam at $z = 0$:

$$v_{b,\max} = \max_{t \in [0,T]} |u_t(0, t)|, \quad T \gg 1,$$

and this quantity was measured in experiments [15]. To find an asymptotic approximation for $\bar{u}$ we first note that due to the fundamental identity of Parseval, one has

$$\|u(\cdot, t)\|^2 = \int_{-H_1}^{H_2} u(z, t)^2 dz \approx \sum_{n=1}^{\infty} |A_n(\epsilon t)|^2.$$

According to (105) at the bifurcation point one has

$$\sum_n A_n(\tau)^2 \approx N_{res}(v) P_1(v).$$

Therefore

$$\bar{u} \approx (N_{res}(v) P_1(v))^{1/2}, \tag{106}$$

for $P_1(v) > 0$, and

$$\bar{u} \approx O(\epsilon) \tag{107}$$

otherwise. To compute $v_{b,\max}$, we use the asymptotic approximation

$$v_{b,\max} \approx \max_t \sum_n \Omega_n A_n(\epsilon t) \cos(\Omega_n t + \phi_n) \psi_n(0) + O(\epsilon).$$

Taking into account that the main contributions in the sum in this approximation are caused by the resonance modes, we obtain that $v_{b,\max}(v)$ and $\bar{u}(v)$ are proportional to the ice rod speed v functions :

$$w_{b,\max}(v) \approx C\, \bar{u} \approx C\, (N_{res}(v) P_1(v))^{1/2},$$

where the constant C does not depend on v.

References

1. Abramain, A.K., Indeitsev, D.A., Bessonov, N.M.: Fluid effect on ice induced vibrations. Proc. Eng. **199**, 1270–1275 (2017)
2. Abramian, A.K., Vakulenko, S.A., van Horssen, W.T.: On a simple oscillator problem describing ice-induced vibrations of an offshore structure. Nonlinear Dyn. **98**, 151–166 (2019)
3. Andrianov, I.V., Manevitch, L.I.: Asymptotology. Mathematics and Its Applications. Springer, New York (2002)
4. Banks, I.T., Inman, D.J.: On damping mechanisms in beams. Trans. ASME **58**(3), 716–723 (1991)
5. Blenkarn K.A.: Measurement and analysis of ice forces on Cook Inlet Structures, Offshore Technology Conference, Houston, TX (1970)
6. Bogoliubov, N., Mitropolsky, Y.A.: Asymptotic Methods in the Theory of Non-Linear Oscillations. Gordon and Breach, New York (1961)
7. De Bruijn, N.: Asymptotic Methods in Analysis. North-Holland, Amsterdam (1961)
8. Dostal, L., Lourens, E.M., Metrikine, A.: Nonlinear model parameter identification for ice-induced vibrations. Proc. Eng. **199**, 583–588 (2017)
9. Gagnon, R.: An explanation for the molikpaq may 12, 1986 event. Cold Reg. Sci. Technol. **82**, 75–93 (2012)
10. Gaiko, N.V., van Horssen, W.T.: Resonances and vibrations in an elevator cable system due to boundary sway. J. Sound Vib. **424**, 272–292 (2018)
11. Hendrikse H.: Ice-induced vibrations of vertically sided offshore structures, Ph.D thesis, TU Delft (2017)
12. Hendrikse, H., Metrikine, A.: Interpretation and prediction of ice induced vibrations based on contact area variation. Int. J. Solids Struct. **75**, 336–348 (2015)
13. Hendrikse, H., Zeemer, G., Owen, C.C.: Experimental validation of a model for prediction of dynamic ice-structure interaction. Cold Reg. Sci. Technol. **151**, 345–358 (2018)
14. Huang, G., Liu, P.: A dynamic model for ice-induced vibrations of structures. J. Offshore Mech. Arct. Eng. **131**, 011501–011506 (2008)
15. Huang, Y., Shi, Q., Song, A.: Model test study of the interaction between ice and a compliant vertical narrow structure. Cold Reg. Sci. Technol. **49**, 151–160 (2007)
16. Indeitsev, D.A., Abramain, A.K., Bessonov, N.M.: Peculiarities of the interaction of a structure with moving ice. Doklady Phys. **61**(11), 555–557 (2016)
17. Ji, X., Oterkus, E.: A dynamic ice-structure interaction model for ice-induced vibrations by using Van der Pol equation. Ocean Eng. **119**, 147–152 (2016)
18. Ji, H., Oterkus, E.: Physical mechanism of ice-structure interaction. J. Glaciol. **64**(244), 197–207 (2018)
19. Jin, D.P., Hu, H.Y.: Ice-induced nonlinear vibration of an offshore platform. J. Sound Vib. **214**(3), 431–442 (1998)
20. Johnson, K.L.: Contact mechanics. Cambridge University Press, Cambridge (1985)
21. Kärna T., Kolari K., Jochmann P., Evers K.U., Bi X.J., et al.: Tests on dynamic ice-structure interaction, 22nd International conference on offshore mechanics and Arctic engineering (OMAE2003), Cancun Mexico (2003)
22. Matlock, H., Dawkins, W.P., Panak, J.J.: Analytical model for ice structure interaction. ASCE J. Eng. Mech. Div. EM **4**, 1083–1092 (1971)
23. Mättänen M.: Numerical model for ice-induced vibration load lock-in and synchronization, In: Proceedings of the 14th International Symposium on Ice, Potsdam/New York/USA, Vol. 2, 923–930 (1998)
24. McKinnon, W.B.: Convective instability in Europa's floating ice shell. Geophys. Res. Lett. **26**(7), 951–954 (1999)
25. McQueen H., Srinil N.: Modelling two-dimensional ice-induced vibrations of offshore structures with geomet-

ric nonlinearities. In: Proceedings of the international conference on offshore mechanics and arctic engineering - OMAE. American Society of Mechanical Engineers (ASME), CAN.,(2015)
26. Muguruma, J., Higuchi, K.: Glaciological Studies on Ice Island T-3. J. Glaciol. **4**(36), 709–730 (1963)
27. Nord, T.S., Lourens, E.M., Oiseth, O., Metrikine, A.: Model-based force and state estimation in experimental ice-induced vibrations by means of Kalman filtering. Cold Reg. Sci. Technol. **111**, 13–26 (2015)
28. Nord, T.S., Lourens, E.-M., Mättänen, M.P., Øiseth, O., Høyland, K.V.: Laboratory experiments to study ice-induced vibrations of scaled model structures during their interaction with level ice at different ice velocities. Cold Reg. Sci. Technol. **119**, 1–15 (2015)
29. Peyton H.R.: Sea ice forces, In: Ice pressures against structures, compiled by Gold, L. and Williams, G. NRC Techn. Memo No. 92, Ottawa, Canada (1968)
30. Sandilo, S.H., van Horssen, W.T.: On a cascade of autoresonances in an elevator cable system. Nonlinear Dyn. **80**, 1613–1630 (2015)
31. Schuster M., Eigen P.: The Hypercycle : a principle of natural self-organization, Berlin (1979)
32. Seidel, M., Hendrikse, H.: Analytical assessment of sea ice-induced frequency lock-in for offshore wind turbine monopiles. Mar. Struct. **60**, 87–100 (2018)
33. Sodhi D.S.: A theoretical model for Ice-Structure Interaction, Proc. of the OMAE-94 conference, ASME, New York, Vol. IV, 29–34 (1994)
34. Takizava, T.: Deflection of a floating see ice sheet induced by a moving load. Cold Reg. Sci. Technol. **11**, 171–180 (1985)
35. Vlasov V.Z., Leont'ev N.N.: Beams, plates and shells on elastic foundations, Israel Program for Scientific Translation, Jerusalem, Israel (1966)
36. Ye, Q., Guo, F., Kärna, T.: Dynamic ice forces of slender vertical structures due to ice crushing. Cold Reg. Sci. Technol. **56**, 77–83 (2009)
37. Ye, K., Li, C., Yang, Y., Zhang, W., Xu, Z.: Research on influence of ice-induced vibration on offshore wind turbines. Renew. Sustain. Energy **11**, 033301 (2019)
38. Zhao, X., Shen, H.: Three-layer viscoelastic model with eddy viscosity effect for flexural-gravity wave propagation through ice cover. Ocean Modell. **131**, 15–23 (2018)
39. Zhu, W.D., Ni, J., Huang, J.: Active control of translating media with arbitrary varying length. J. Vib. Acoust. **123**, 347–358 (2001)